

# Using Selected Combining Algorithm for Blood Pressure Measurement in Micro MW-PPG Sensor

Wu, Chien-Ta, Department of Electrical Engineering, National Taipei University of Technology.

Wang, Ta-Wei, Department of Electrical Engineering, National Taipei University of Technology.

Chang, Cheng-Chun, Associate Professor, Department of Electrical Engineering, National Taipei University of Technology.

**Abstract**—With the rapid development of medical technology and the effects of aging, the issues related to medical care and long-term care have become extremely important. Among much physiological information, blood pressure is one of the important factors, while traditional medical instruments for blood pressure measurements are usually not portable. In this paper, the developed multi-wavelength PPG (MW-PPG) measurement module is used to collect multi-wavelength PPG signals. Three light sources with spectra range in red, green and infrared-red are used to collect 15 MW-PPG signals. A Signal-to-Noise Ratio based (SNR-based) selected combining algorithm is proposed to select the PPG signal with the best signal quality. The selected MW-PPG signals with the corresponding neural network model are used for blood pressure prediction.

In this paper, we show that based on the proposed SNR-selected combining algorithm to select the PPG wavelength for blood pressure measurement on different objects, compared to using the green PPG signal, averagely 5% MAE can be reduced in diastolic and systolic blood pressure measurement. Further, a clinical trial was conducted on 10 subjects. The results of the clinical trial show that the SNR-based selected combining algorithm could reduce the prediction error by up to 12% compared to the single wavelength PPG sensing methodology.

**Index Terms**—blood pressure prediction, multi-wavelength PPG technique, machine learning, transfer learning.

## I. INTRODUCTION

**T**HANKS to the rapid development of embedded systems, big data analysis, and artificial intelligence in recent years, modern medicine is gradually moving towards to precision medicine. Various physiological signals such as heart rate, blood pressure, and blood sugar are continuously monitored through the wearable devices and collected into a huge database in order to build a medical big data system. Furthermore, artificial intelligence and machine

learning algorithms are used to train prediction models, marking the beginning of preventive healthcare. In response to the recent COVID-19 outbreak, the healthcare metrics measured by personalized smart wearable devices are considered indicators of COVID-19 infection and assessment. Since the COVID-19 virus affects the nervous system's sensitivity to oxygen, the brain may fail to detect hypoxia in real-time, leading to invisible hypoxia (happy hypoxia) [1], which can delay medical treatment and miss the golden period for intervention. Wearable devices can monitor patients' blood oxygen levels in real-time and provide appropriate medical measures to reduce the mortality caused by COVID-19.

Photoplethysmography (PPG) has become widely used in wearable devices as a convenient method for heart rhythm and blood oxygen measurement. In recent years, the miniaturization of electronic components and the rapid development of PPG sensing modules have significantly contributed to the development of PPG applications for blood pressure measurement. Traditionally, many studies have pointed out that the distance between the PPG sensing signal and the peak of the ECG can serve as the pulse transit time (PTT). Given the linear relationship between PTT and blood pressure, it is believed that PTT can be used to infer blood pressure values. However, the limited number of features and the requirement for using a large ECG measurement device alongside hinder the accuracy of blood pressure prediction and make portable monitoring inconvenient. In 2005, Nitzan et al [2] demonstrated that the PPG signals from different body parts can be captured and the time difference between the peaks of the PPG signals can be used as the PTT to predict blood pressure. However, the sensor must be carried on different body parts, which makes it inconvenient to carry. After 2009, many researchers [3][4] have focused on extracting multiple features from single-wavelength PPG signals for blood pressure measurement. The number of

This work was supported by the National Science and Technology Council (NSTC) (NSTC112-2740-B-001-004). Corresponding author: C.C., Chang. (email: [ccchang@mail.ntut.edu.tw](mailto:ccchang@mail.ntut.edu.tw)).

C.T., Wu. was with Department of Electrical Engineering, National Taipei University of Technology, Taiwan.

T.W., Wang. was with Department of Electrical Engineering, National Taipei University of Technology, Taiwan.

extracted features has gradually increased from 4 to 21, resulting in prediction errors of less than 4%. This innovation in PPG application for blood pressure measurement represents a significant advancement.

However, many studies have pointed out that the captured PPG sensing signals are susceptible to environmental variables such as skin surface relaxation [5], skin color [6], skin surface temperature [7], etc. To obtain stable signal quality, MW-PPG sensing technology has been increasingly recognized in recent years. Since PPG signals of different wavelengths can penetrate different skin depths [8]-[11], Zhang et al [12] pointed out in 2019 that short-wavelength PPG signals have a higher Signal-to-Motion Artifacts Ratio (SMR) compared to long-wavelength PPG signals. Consequently, short-wavelength PPG signals can serve as the primary signal, while long-wavelength PPG signals are more susceptible to dynamic noise. By utilizing spectrum analysis, dynamic noise can be extracted and subtracted from the main signal to obtain a more stable PPG signal. Chang et al [13] also used a micro spectrometer sensor chip to develop an MW-PPG measurement device in 2019. The developed signal processing algorithm could robustly extract heart rhythm and blood oxygen detection values, thereby validating the feasibility of MW-PPG for blood pressure sensing. In 2020 [14], they further validated that PPG signals of different wavelengths in different postures can provide varying signal-to-noise ratios (SNRs). By implementing a signal combining algorithm, wearers can merge PPG signals with high SNRs from MW-PPG sensors in different postures. On average, MW-PPG signals exhibit a 28% higher SNR than conventional single-wavelength PPG signals across different postures.

The MW-PPG measurement module established in our previous studies [13] was utilized in this paper to collect MW-PPG signals and explore the selection of PPG signal bands for different subjects using a selected combining algorithm to achieve blood pressure measurement via neural network. Regarding neural network training in this study, we employed the transfer learning algorithm due to the challenges in collecting medical data. Transfer learning enables the transfer of experience, knowledge, and features learned from a neural network trained on a source dataset to a model for a target dataset. In our research, the publicly available MW-PPG signals database, MIMIC-III Waveform Database, served as the source dataset to pre-train the neural network model, which was then transferred to the model for the target dataset collected by the developed MW-PPG measurement module. MIMIC (Medical Information Mart for Intensive Care) is a large, freely-available database comprising deidentified health-related data from patients who were admitted to the critical care units of the Beth Israel Deaconess Medical Center. MIMIC-III contains data from 2001-2012. The data was collected from Metavision and CareVue bedside monitors.

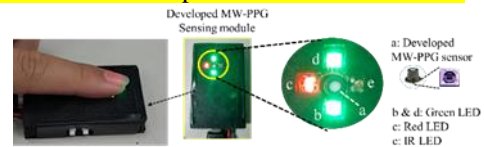
## II. BACKGROUND KNOWLEDGE

Section 2.1 introduces the architecture and principles of the developed MW-PPG measurement module. Section 2.2 discusses various feature extraction methods for blood pressure prediction, while Section 2.3 presents the development of neural networks and

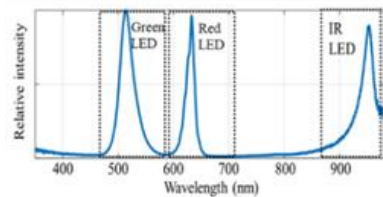
transfer learning in the field of artificial intelligence.

### A. Micro MW-PPG Measurement Module

The MW-PPG measurement module used in this paper is shown in Figure 1(a). The light sources are arranged symmetrically, with the MW-PPG sensor positioned in the center. This arrangement allows for the reflection of light from different wavelengths by the skin, gathering at the center to facilitate MW-PPG signal collection. Three sets of LEDs serve as the light source, which are green light (wavelength 515 nm), red light (wavelength 660 nm), and infrared light (wavelength 940 nm), and the spectra of the three light sources are shown in Figure 1(b). The nanoLambda micro spectrometer is used as the receiver side sensor for MW-PPG signal detection. Unlike conventional spectrometers, which often occupy several square centimeters, this sensor is significantly smaller, only occupying a few square microns. It achieves this compact size by eliminating precision optical components such as gratings and focal lenses. The sensor can collect 15 wavelengths of PPG signals simultaneously, including 505nm, 510nm, 515nm, 520nm, 525nm, 620nm, 625nm, 630nm, 635nm, 640nm, 930nm, 935nm, 940nm, 945nm, and 950nm. Compared to conventional photo-diodes (PDs) that obtain PPG signals of different wavelengths through time-sharing and multiplexing via a switch, and then recombine these signals into multi-wavelength PPG signals, the MW-PPG measurement module used in this paper can directly resolve PPG signals of multiple wavelengths simultaneously. This eliminates the need for signal recombination, enabling true real-time MW-PPG signals. As demonstrated in a previous study [13], this measurement module offers the advantage of simultaneous and robust measurement compared to conventional PDs.



(a) NSP32 multi-wavelength PPG measurement module



(b) The spectra of the three light sources

Fig. 1. Pictorial and used spectra of the light source in the MW-PPG measurement module

The mathematical model of the MW-PPG sensing device in this study is shown in Figure 2. The PPG sensor signal at each wavelength captured by the micro MW-PPG sensor can be expressed as

$$y_t = F_t x_t^T + n_t \quad (1)$$

where  $y_t = [y_{1,t} \ y_{2,t} \ \dots \ y_{L,t}]$ , and  $y_{i,t}$ ,  $i = 1, \dots, L$  is the PPG sensing signal collected at time  $t$  for the  $i$ -th wavelength,

$$F = [f_1^T \ f_2^T \ \dots \ f_L^T] \quad (2)$$

where  $f_i^T, i = 1, \dots, L$  is the response curve of the  $i$ -th sensing wavelength. In this study, we assume that the response curve of a sensing wavelength is an approximately perfect Gaussian curve,  $x_t$  is the reflected spectrum received by the sensor, and  $n_t$  is the noise component of the received signal.

From [15], the PPG sensing signal at each wavelength can be divided into the signal  $x$  (freq.<7 Hz) and noise  $n$  (freq.>7 Hz) components. The signal component is used for the feature extraction and model training, and the signal and noise components are used to calculate the SNR values, which are used to evaluate the signal selection at each wavelength.

$$y_t = s_t + n_t \quad (3)$$

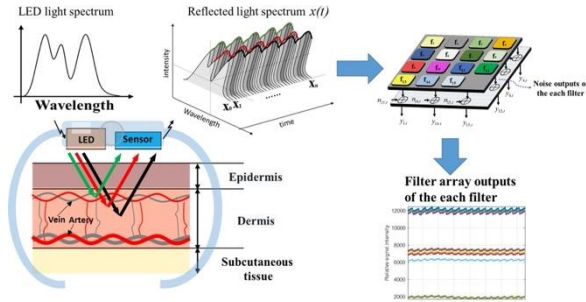


Fig. 2. Mathematical model of MW-PPG sensing device

### B. PPG Blood Pressure Feature Extraction

The association between PPG signals and blood pressure has been studied extensively. PPG signals can record pulsatile changes in blood flow in subcutaneous vessels during each heartbeat. These changes in the waveform are related to cardiac blood transfusion, vessel shape, and vessel wall condition. Therefore, many studies have been conducted to predict blood pressure by analyzing the features of the PPG waveform in various ways.

In the frequency domain, Xing et al [16] used the data in MIMIC II to extract the amplitude and phase in the waveform by FFT transformation. MIMIC-II contains data from 2001-2008. The data was collected from CareVue bedside monitors. MIMIC-II is no longer publicly available but the data can still be obtained from MIMIC-III by only including data from the CareVue monitors. They concluded that this method is more stable than extracting features from the time domain because there is no need to capture the location of particular time points, and multiple periodic pulse signals can be analyzed at one time. Subsequently, the Levenberg-Marquardt algorithm in ANN was used to train the amplitude and phase as features, and the final predicted results were  $-1.67 \pm 2.46$  mmHg for SBP and  $-1.29 \pm 1.71$  mmHg for DBP.

In the time domain, as shown in figure 3, Suzuki et al [3] calculated the turning points on a single PPG waveform by quadratic differentiation and recorded the four main turning points PW, TW, Dn, and DW on the PPG waveform as characteristic parameters and predicted the SBP values by the Error-Correcting Output Codes (ECOC) method. The predicted results were  $r=0.75$ ,  $MD=-1.2$  [mmHg], and  $SD=11.7$  [mmHg]. In addition, Kurylyak et al [4] concluded that the feature point of the PPG waveform is the time difference between peak and trough in a single pulse, and the time difference at each pulse

height is considered as the variation of blood flow with the pulsation of the heart, and based on the characteristics adopted in other previous papers: the horizontal distance of the pulse at pulse heights of 10% [17], 50% and 66% [18]. To fully express the pulse information, 25%, 33%, and 75% were added as feature parameters. In this study, 21 features extracted from a single PPG waveform are used as input to the neural network model, and the MIMIC database data was used for training data. As a results, absolute error  $3.80 \pm 3.46$ (mmHg) and  $2.21 \pm 2.09$ (mmHg) for SBP and DBP can be achieved.

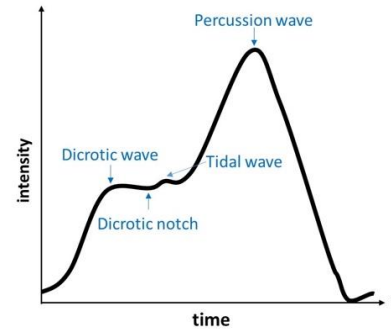


Fig. 3. Basic feature of PPG signal in time-domain

### C. Neural Networks And Transfer Learning

With the development of technology, AI have been gaining attention from the public, among which Artificial Neural Network (ANN) is a mathematical model that imitates the structure and function of the human brain, being used to perform regression and classification. The number of neuron features that can be trained increases as the computing speed and performance of the graphics chip increase, allowing the neural network model to achieve better learning results.

The amount of training data is always the key to deciding whether a model is good or bad, but not all data acquisition methods are simple. Especially in the medical field, it is not easy to collect each piece of data. To solve these problems, some researchers have developed transfer learning methods as shown in Figure 4. Transfer learning is a special area of research in machine learning, and its research is based on the idea so that when humans encounter a new problem, they can solve the new problem faster and more efficiently based on their previous experience and knowledge, which is a process of transferring knowledge. Therefore, as long as a model with the same or related task as the neural network model to be trained can be found, it can be used as the source domain model and the target domain model can be trained by transfer learning, instead of collecting enough data, labeling data and training the model on the target domain from scratch, which greatly saves the time of data collection.

In this paper, due to the limited amount of data that can be collected using the MW-PPG sensor, the results of neural network model training are usually unsatisfactory, so the MIMIC public database data are used as the training data to train neural network with source domain knowledge. The source domain neural network model is used as the initial model to train with the collected data from the MW-PPG sensor.

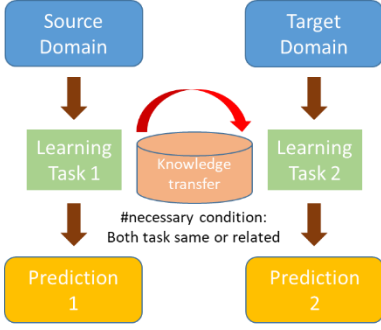


Fig. 4. Transfer learning method

### III. PROPOSED ALGORITHM FOR MW-PPG BLOOD PRESSURE MEASUREMENT

#### A. Pre-processing of the Signal

Before the feature capture, there are many noises generated in the circuit operation such as thermal noise, white noise, shot noise, etc. Generally, the frequency of heartbeat is between 60 and 100 (bpm), so it can be seen that the frequency range of the PPG signal is about 0.5~7Hz [15], as shown in Figure 5. To obtain the PPG sensing signal without noise, the raw PPG sensing signal  $y$  at time  $t$  is filtered by a bandpass filter to remove the high and low-frequency noise (Fstop1:0.1708 Hz, Fstop2:6 Hz, Fpass1:0.9 Hz, Fpass2:7 Hz). The raw PPG sensing signal passed with a bandpass filter can be expressed as  $\tilde{y}_{i,t}$ .

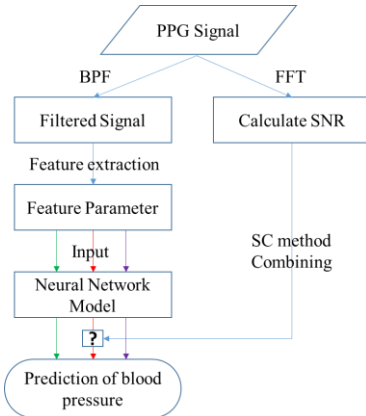


Fig. 5. Data pre-processing method

Next, the feature extraction technique in Section 2.2 is used to extract 21 feature parameters from the noise-filtered PPG sensing signal, including CP (Cardiac Period), SUT (Systolic upstroke Time), DT (Diastolic Time), 6 parameters of DW (Diastolic Width), 6 parameters of SW (Systolic Width) + DW, and 6 parameters of DW/SW, as shown in Figure 6. In addition, we further extend the method by including the 6 SW values as feature parameters for training.

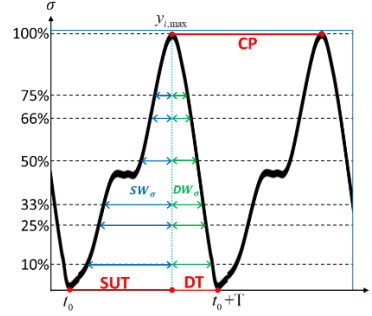


Fig. 6. PPG signal feature extraction

Since [4] holds that the feature point of the PPG waveform is the time difference between the peak and the trough in a single pulse, the time difference under each pulse height  $\sigma$  emerges as the change of blood flow with the heartbeat. In this study, according to [4], the reference points of the PPG waveform are used as feature parameters, where each feature parameter is calculated by the following mathematical equations.

Following (2) and (3), a single pulse of PPG signal can be expressed as

$$\tilde{y}_{i,t \rightarrow t_0+T}(\text{miss } i) \quad (4)$$

where  $t_0$  is the start time of a single pulse,  $T$  is the period of the PPG signal. In the  $i$ -th wavelength signal, the peak value  $y_{i,max}$  of the single pulse and the peak time point  $t_{i,max}$  can be expressed as

$$\begin{cases} y_{i,max} = \max_{t \in [t_0, t_0+T]} \tilde{y}_{i,t} \\ t_{i,max} = \text{arg} \max_{t \in [t_0, t_0+T]} \tilde{y}_{i,t} \end{cases} \quad (5)$$

SUT and DT represent the time differences from peak to trough, and the time difference from the peak of one pulse wave to the peak of the next pulse wave in the cycle, respectively. These parameters can be expressed as

$$\begin{cases} SUT = t_{i,max} - t_0 \\ DT = (t_0 + T) - t_{i,max} \\ CP = t_{i,max}(T + 1) - t_{i,max}(T) \end{cases} \quad (6)$$

In addition,  $SW_\sigma$  and  $DW_\sigma$  represent the peak height of the pulse at each ratio  $\sigma$ . The time difference from the peak can be expressed as

$$\begin{cases} SW_\sigma = t_{i,max} - t_{start,\sigma} \\ DW_\sigma = t_{end,\sigma} - t_{i,max} \end{cases} \quad (7)$$

where  $t_{start,\sigma}$  and  $t_{end,\sigma}$  represent the time points closest to the value of  $y_\sigma$  in the left and right sides of the wave peak.

$$\begin{cases} t_{start,\sigma} = \arg \min_{\substack{t \in [t_0, t_0+T] \\ t \leq t_{i,max}}} |y_{i,t} - y_\sigma| \\ t_{end,\sigma} = \arg \min_{\substack{t \in [t_0, t_0+T] \\ t \geq t_{i,max}}} |y_{i,t} - y_\sigma| \end{cases} \quad (8)$$

and  $y_\sigma$  is the peak height of the pulse at different ratios of  $\sigma$ .

$$\begin{cases} y_\sigma = \sigma \cdot y_{i,max} \\ \sigma = 0.1, 0.25, 0.33, 0.5, 0.66, 0.75 \end{cases} \quad (9)$$

As a result, the 27 features  $\varepsilon$  can be extracted from (4) to (9).

$$\varepsilon = \left[ CP, SUT, DT, SW_\sigma, DW_\sigma, SW_\sigma + DW_\sigma, \frac{DW_\sigma}{SW_\sigma} \right]$$

### B. Neural Network Model Training

The 27 features are used as the input to the neural network model. In this neural network model framework, the mean square error (MSE) is used for the loss function, Adam is used for the optimizer, and a multilayer perceptron (MLP) framework with 6 hidden layers is used for training. In addition, for the target domain neural network model, the data augmentation method is used to avoid the lack of data in the target domain and the excessive computation caused by training 15 different wavelengths of neural network models. The sensor uses three types of LED light sources: green, red, and infrared, each of which captures five PPG signals of similar wavelengths as the same set of target domain data. The green wavelength bands 505nm, 510nm, 515nm, 520nm, and 525nm are considered the same group. The red wavelengths 620nm, 625nm, 630nm, 635nm, and 640nm are considered the same group. Infrared wavelengths 930nm, 935nm, 940nm, 945nm, and 950nm are considered the same group. The parameters of Layers 1 and 2 are retained, and the parameters of other layers are fixed. And then the data measured in the MIMIC database are transferred to the three separate green, red, and infrared target field neural network models using the layer transfer method.

### C. SNR-based Selected combining Algorithm

In this study, the PPG signal wavelength with the best signal-to-noise ratio (SNR) is selected as the wavelength band for blood pressure prediction by a selected combining algorithm. Since the selected combining algorithm has been widely used in the field of MIMO communication, this study applies this theory to select three types of green, red, and infrared neural network models. In this study, the SNR is calculated as follows: after converting the time domain signal to the frequency domain signal, the normal PPG signal frequency is 0.5Hz~7Hz, where freq.<7 Hz is defined as signal and freq.>7 Hz is defined as noise, and the SNR is calculated by dividing the signal power by the noise power. The strength of SNR means the stability of the waveform in the PPG signal, and the selection of the PPG signal wavelength with the best SNR means that the PPG signal with better signal quality can be used for prediction.

Through the selected combining algorithm, the predicted blood pressure values of each wavelength can be merged into

one predicted blood pressure value by the algorithm, and the mathematical equation can be expressed as

$$SC_{method}(SBP, DBP) = \sum_{i=1...L} \omega_i (SBP_i, DBP_i) \quad (10)$$

$$\omega_i = \begin{cases} 1, snr_i = \max_{i=1...M} (snr_i) \\ 0, otherwise \end{cases} \quad (11)$$

where  $\omega_i$  is the weight of the  $i$ -th wavelength, SNR is the signal-to-noise ratio, and the mathematical equation can be expressed as

$$snr_i = \frac{E[s_i^2(t)]}{E[n_i^2(t)]} = \frac{\sum_{f \leq 7Hz} s_i^2(f)}{\sum_{f > 7Hz} n_i^2(f)} \quad (12)$$

As shown in Figure 7, a 20-second MW-PPG sensing signal was collected, and the SNRs of red, green, and infrared light were 31.52(dB), 18.90(dB), and 26.57(dB), respectively. In addition, Figure 7(b) shows that the waveform of the red PPG sensor signal is clearer than those of the green and infrared signals. Given this, the SNR-based selected combining algorithm was used to select the blood pressure prediction results of the red PPG signal with better SNR. Besides, the mean absolute error (MAE) of the red PPG signal was 5.18 (mmHg). Furthermore, the prediction errors of green and infrared light were MAE 15.25(mmHg) and MAE 8.47(mmHg), respectively, which further verified that the signal quality and the prediction error of blood pressure were positively correlated.

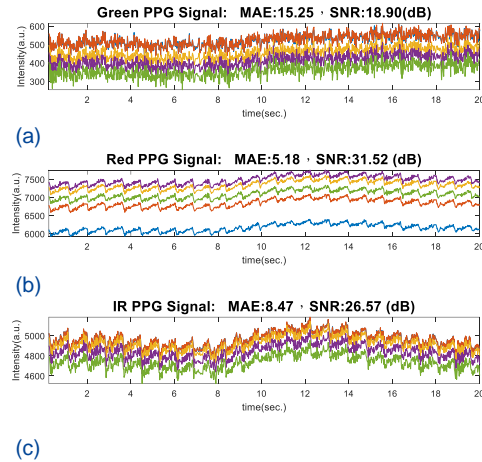


Fig. 7. A set of 20-second measurement signals of the micro MW-PPG measurement module, where (a) is the measurement signal with a wavelength from 505 nm to 525 nm, (b) is the measurement signal with a wavelength from 620 nm to 640 nm, and (c) is the measurement signal with a wavelength from 930 nm to 950 nm.

## IV. EXPERIMENTAL RESULTS

### A. Experimental Data Collection and Test Results

In this study, the micro multi-wavelength MW-PPG blood pressure monitor introduced in Section 2 is used for research sampling and data collection with 89 MW-PPG signals collected, and each MW-PPG signal contains 15 bands, including red band (505, 510, 515, 520, 525 nm), green band (620, 625, 630, 635, 640 nm), and infrared band (940, 945, 950, 955, 960 nm). Given the difficulty of data collection for human experiments, five close wavelengths of the same light source are used to train the blood pressure measurement model for that

color to realize the increase in the amount of data collection through the expansion of the data. In addition, each MW-PPG sensing signal is collected for 20 seconds for signal-to-noise ratio analysis. During the collection process, a commercially available cuff blood pressure monitor (OMRON HEM-7121) is used to measure the diastolic and systolic blood pressures of the subjects as ground truth. The systolic blood pressure range of the subjects in this study is 63-88 mmHg, and the diastolic blood pressure is 81-133 mmHg.

The architecture of the blood pressure measurement model for each wavelength is shown in the following table. In order to avoid overfitting due to the small data set collected, migration learning was used to train the original model using a total of 12,500 data from the public database (MIMIC III), as shown in Table 1. Then, Layer 6 and the output layer were used as the migration layer. The target model was trained with 70%, 15%, and 15% of the collected data as training data, validation data, and test data for micro multi-wavelength blood pressure monitors.

**TABLE I**  
SW PPG BP ARCHITECTURE FOR EACH  
RED, GREEN, AND INFRARED PPG SIGNALS

Layer	Operator
1	FC 27x256 + ReLU
2	FC 256x256 + ReLU
3	FC 256x256 + ReLU
4	FC 256x256 + ReLU
5	FC 256x128 + ReLU
6	FC 128x64 + ReLU
7	FC 64x2

For the data testing, 89 data were collected and tested. Figure 8 shows the mean absolute errors of the systolic and diastolic pressure measurements in different ways for each test data. The red, green, and blue lines are the measured MAE of the blood pressure when using red, green, and infrared red PPG signals, respectively, and the black line is the MAE when the PPG signal selected according to the proposed SNR of -based selective combining algorithm. It is worth noting that the wavelength of the minimum MAE varies from measurement data to measurement data, which is explained in Section 1. Therefore, the wavelength of PPG signal with optimal SNR also varies for different measurements. In terms of systolic pressure, the MAE was 6.7(mmHg), 7.2(mmHg), and 6.47(mmHg) for red, green, and infrared light, respectively. If the light source with the lowest MAE is selected for each measurement, the average MAE can reach 5.1(mmHg). On the other hand, 6.13(mmHg) MAE can be achieved by using the selected combining algorithm proposed in this study, which can reduce the error by 9.2%, 17.4%, and 5.5% compared to green light, infrared light, and red light, respectively. Furthermore, for diastolic blood pressure, the MAE 4.79(mmHg), 4.98(mmHg), and 4.54(mmHg) for the infrared, green, and red lights are achieved, respectively. If the light source with the lowest MAE is selected for each measurement, the average MAE can reach 3.61(mmHg). Compared to that, the 4.53(mmHg) MAE can be achieved by using the selected combining algorithm proposed in this study, which can reduce the error by 5.7%, 9.9%, and 0.2% compared to green, red, and infrared lights respectively. It can be seen that although the selected combining algorithm

can not always select the wavelength with lowest MAE, while based on the SNR as reference, we can dynamically select the wavelength for blood pressure measurement which is not the worst. As a result, compared to using the green PPG signal for the blood pressure measurements, the averaged MAE of systolic and diastolic pressures can be reduced up to 5% when the proposed SNR-based selected combining algorithm is used.

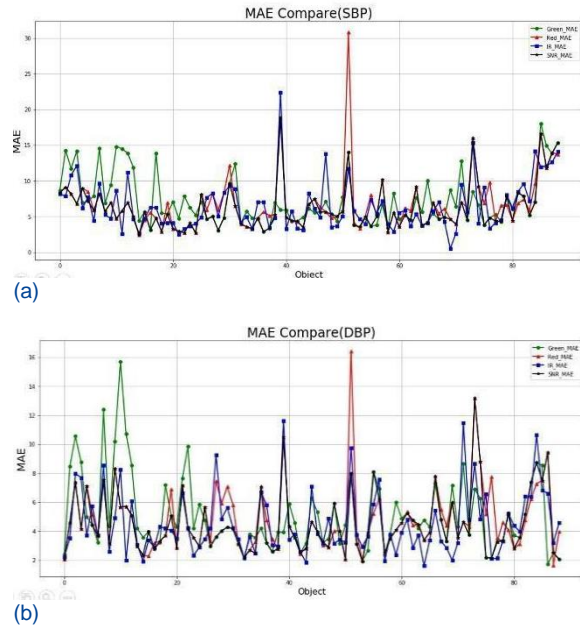


**Fig. 8.** MAE of (a) SBP and (b) DBP for 89 measurements with the use of red, green, and IR lights and the proposed SNR-based selected merged PPG signals.

## B. Clinical Test Results

In this study, the developed micro MW-PPG sensing device was further tested on ten subjects in the clinical setting, as shown in Figure 9, where (a) and (b) show the systolic and diastolic MAE respectively measured by different light sources in the micro MW-PPG sensing device for the ten subjects. The red, green, blue, and black lines are the results of the MW-PPG sensing device using red, green, infrared, and SNR-based algorithms, respectively. It is noteworthy that the MAE of systolic and diastolic pressures are different for the same light source in the same subject. For example, the diastolic MAE of Subject 5 was 2.59(mmHg), 3.59(mmHg), and 4.73(mmHg) under red, green, and infrared light, respectively, and the systolic MAE was 6.71(mmHg), 5.85(mmHg), and 6.96(mmHg) under red, green, and infrared light, respectively. The MAE of red light was found to be the best in diastolic blood pressure, better than green light at 1 (mmHg) and infrared light at 2.14 (mmHg), while the MAE of green light was the best in diastolic blood pressure, better than red light at 0.86 (mmHg) and infrared light at 1.11 (mmHg). If the green light is selected for blood pressure measurement, although more accurate results can be obtained for diastolic blood pressure, there is a loss of 1(mmHg) in accuracy for systolic blood pressure compared to red light in MAE. In contrast, if the red light is selected for blood pressure measurement, although the lowest measurement error is obtained in systolic pressure, there is a loss in accuracy

of 0.86(mmHg) in diastolic pressure compared to green light in MAE. Therefore, as described in Section 1 of this paper, due to the differences in the nature of the skin of different subjects and various environmental variables, the light source suitable for systolic and diastolic blood pressure measurements will change accordingly. Therefore, the selection of an appropriate light source for blood pressure measurement is a major challenge for different subjects.

Compared with the measurement method using only a single light source, the SNR-based selected combining algorithm proposed in this paper can select the best results in terms of the average MAE of systolic and diastolic pressures among different subjects. For example, for Subject 5, the average MAE of the red light source selected by the SNR-based selected combining algorithm was better than that of the green light (4.72 mmHg) and infrared light (5.85 mmHg). In addition, among all 10 subjects, the results of the proposed selected combining algorithm were used to select the lowest average MAE for 5 subjects and the next best average MAE for the remaining 5 subjects. The SNR-based selected combining algorithm by signal quality profiling does not guarantee the selection of the source with the lowest average MAE, but it can relatively select the source with 50% of the best and 50% of the second best MAE.

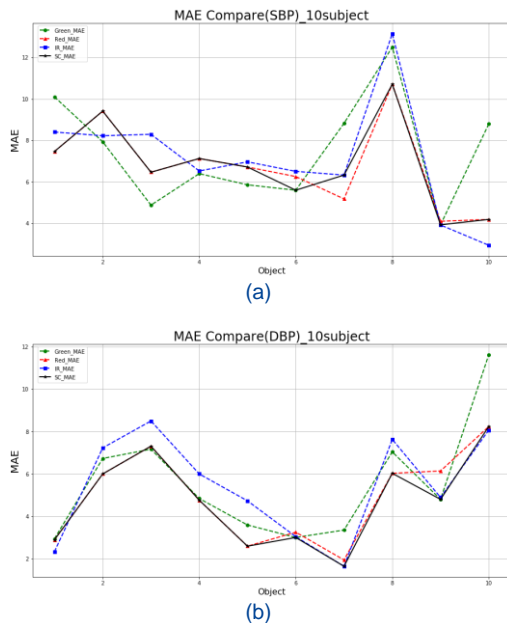


Fig. 9. MAE of (a) SBP and (b) DBP for 10 clinical test measurements with the use of red, green, and IR lights and the proposed SNR-based selected merged PPG signals.

## V. CONCLUSIONS

In this study, based on the micro MW-PPG measurement module developed in [13], 15 sets of wavelengths of MW-PPG signals were collected from three light sources, and the blood pressure measurement models were trained under each light source by transfer learning and deep learning algorithms. The SNR-based selected combining algorithm was used to select the light source with the best signal quality and to predict blood pressure by the corresponding neural network model. This

method achieves an average error improvement of up to 5% in diastolic blood pressure. In addition to the training dataset and the test dataset, ten clinical tests were also collected to determine the quality of blood pressure. The average MAE of green, infrared, and red light was 5.75(mmHg), 6.09(mmHg), and 5.51(mmHg), respectively, and the SNR-based selected combining algorithm was further validated to reduce the prediction error through clinical testing. The MAE could reach 5.33(mmHg) if the selected combining algorithm proposed in this paper is used, which can reduce the error by up to 12% compared to the single light source.

All experiments and data collection were performed under the supervision of the Chang Gung Medical Foundation Institutional Review Board.

## REFERENCES

- [1] M. Uginet, G. Breville, F. Assal, K.-O. Lövblad, M. I. Vargas, J. Pugin, J. Serratrice, F. R. Herrmann, P. H. Lalive, G. Allali, "COVID-19 encephalopathy: Clinical and neurological features," *Wiley Journal of Medical Virology*, vol. 93, no. 7, pp. 4374-4381, July 2021.
- [2] M. Nitzan, C. Rosenfeld, A. T. Weiss, E. Grossman, A. Patron and A. Murray, "Effects of external pressure on arteries distal to the cuff during sphygmomanometry," *IEEE Transactions on Biomedical Engineering*, vol. 52, no. 6, pp. 1120-1127, June 2005.
- [3] S. Suzuki and K. Oguri, "Cuffless blood pressure estimation by error-correcting output coding method based on an aggregation of AdaBoost with a photoplethysmograph sensor," in *proc. of 2009 Annu. Int. IEEE EMBS Conf.*, Minneapolis, MN, 2009.
- [4] Y. Kurylyak, F. Lamona and D. Grimaldi, "A neural network-based method for continuous blood pressure estimation from a PPG signal," in *proc. of 2013 IEEE I2MTC*, Minneapolis, MN, pp. 280-283, 2013.
- [5] J Liu et al. "Multi-wavelength photoplethysmography method for skin arterial pulse extraction." *Biomedical optics express*, vol. 7, no. 10, pp. 4313-4326, Sep. 2016.
- [6] L. Yan, S. Hu, A. Alzahrani, S. Alharbi and P. Blanos, "A multi-wavelength opto-electronic patch sensor to effectively detect physiological changes against human skin types," *Biosensors*, vol. 7, no. 2, pp. 1-12, June 2017.
- [7] Y. Maeda, M. Sekine, T. Tamura, A. Moriya, T. Suzuki and K. Kameyama, "Comparison of reflected green light and infrared photoplethysmography", in *proc. of 30th Annu. Int. IEEE EMBS Conf.*, pp. 2270-2272, Aug. 2008.
- [8] J. Lee, K. Matsumura, K. Yamakoshi, P. Rolfe, S. Tanaka and T. Yamakoshi, "Comparison between red, green and blue light reflection photoplethysmography for heart rate monitoring during motion," the 35th Annual International Conference of the IEEE Engineering in Medicine and Biology Society (EMBC), pp. 1724-1727, Osaka, 2013.
- [9] J. Spigulis, L. Gailite, R. Erts and A. Lihachev, "Contact probe pressure effects in skin multi-spectral photoplethysmography," *European Conference on Biomedical Optics*, pp. 307-314, Munich, 2007.
- [10] L. Yan, S. Hu, A. Alzahrani, S. Alharbi and P. Blanos, "A multi-wavelength opto-electronic patch sensor to effectively detect physiological changes against human skin types," *Biosensors*, vol. 7, no. 2, pp. 1-12, Jun. 2017.
- [11] Y. Maeda, M. Sekine, and T. Tamura, "The advantages of wearable green reflected photoplethysmography," *Journal of Medical Systems*, vol. 35, no. 5, pp. 829-834, Oct. 2011.
- [12] Y. Zhang et al. "Motion artifact reduction for wrist-worn photoplethysmograph sensors based on different wavelengths," *Sensors*, vol. 19, no 3, pp.673, Feb. 2019.
- [13] C. C. Chang, C. T. Wu, B. I. Choi and T. J. Fang, "MW-PPG sensor: An on-chip spectrometer approach," *Sensors*, vol. 19, no. 17, pp. 3698, 2019.
- [14] S.-H. Chen, Y.-C. Chuang and C.-C. Chang, "Development of a Portable All-Wavelength PPG Sensing Device for Robust Adaptive-Depth Measurement: A Spectrometer Approach with a Hydrostatic Measurement Example," *Sensors*, vol. 20, no. 22, pp. 1-12, Nov. 2020.
- [15] M. Elgendi, "C, E and D Waves Detection in the Acceleration Photoplethysmogram," *Computer Methods and Programs in Biomedicine*, vol. 117, no. 2, pp. 125-136, 2014.

- [16]Xing, Xiaoman; Sun, Mingshan (2016). Optical blood pressure estimation with photoplethysmography and FFT-based neural networks. *Biomedical Optics Express*, 7(8), 3007–. doi:10.1364/BOE.7.003007
- [17]S. Linder, S. Wendelken, E. Wei, and S. McGrath, “Using the morphology of photoplethysmogram peaks to detect changes in posture,” *Journal of Clinical Monitoring and Computing*, vol.20(3), pp.151–158, June 2006.
- [18]X. F. Teng and Y. T. Zhang, “Continuous and noninvasive estimation of arterial blood pressure using a photoplethysmographic approach,” *Proc. of 25th Annual Inter. Conf. of the IEEE Engineering in Medicine and Biology Society*, Cancun, Mexico, 2003, pp. 3153 – 3156.



**Chien-Ta, Wu.** and all authors may include biographies if the publication allows. Biographies are often not included in conference-related papers. Please check the Information for Authors to confirm. Author photos should be current, professional images of the head and shoulders. The first

paragraph may contain a place and/or date of birth (list place, then date). Next, the author’s educational background is listed. The degrees should be listed with the type of degree in what field, which institution, city, state, and country, and year the degree was earned. The author’s major field of study should be lowercase.

The second paragraph uses the preferred third person pronoun (he, she, they, etc.) and not the author’s last name. It lists military and work experience, including summer and fellowship jobs. Job titles are capitalized. The current job must have a location; previous positions may be listed without one. Information concerning previous publications may be included. The format for listing publishers of a book within the biography is: *Title of Book* (publisher name, year) similar to a reference. Current and previous research interests end the paragraph.

The third paragraph begins with the author’s preferred title and last name (e.g., Dr. Smith, Prof. Jones, Mr. Kajor, Ms. Hunter, Mx. Riley). List any memberships in professional societies other than the IEEE. Finally, list any awards and work for IEEE committees and publications.

**Ta-wei, Wang.** photograph and biography not available at the time of publication.

**Cheng-Chun, Chang.** photograph and biography not available at the time of publication.